Driven Odd Elasticity in Passive Mechanical Metamaterials

Mohamad Rahimi* and Harold S Park†
Department of Mechanical Engineering, Boston University, 02215, Boston, MA, USA

We present a mechanical mechanism leveraging passive mechanical components, i.e. chiral gears and a square lattice metamaterial, to demonstrate driven odd elasticity in a mechanical metamaterial. The mechanism couples tension and shear in a non-reciprocal way, resulting in an odd shear modulus. The emergence of this odd shear modulus enables non-conservative work in a standard quasistatic strain cycle, and further enables the non-Hermitian skin effect in dynamics. Our results demonstrate that odd elasticity can be achieved in mechanical structures using passive elements without electronic components coupled with feedback or robotic control systems.

The behavior of a linear elastic isotropic solid can be described by a free energy function, and therefore such solids conserve linear and angular momentum and energy, and are mechanically passive, i.e. they cannot do work on their surroundings [1]. Furthermore, the constitutive relations that describe the stress-strain relationships of such solids are symmetric, or reciprocal, and satisfy the well-known Maxwell-Betti reciprocity [2–4]. Recently, the concept of an odd elasticity was theoretically introduced [5] to describe linear elastic isotropic solids whose mechanical behavior cannot be described by a free energy function. As a result, odd elastic solids have a non-symmetric elasticity tensor that captures nonreciprocity, where the mechanical response to different loads is not the same. For example, in an odd elastic solid, extension could induce torque, while the same torque would not induce extension [5]. A 2D odd elastic solid is also chiral, so it cannot be superimposed on its mirror transformation through any translation or rotation, which enables the coupling of different deformation fields (i.e. tension to shear) that would otherwise require anisotropy to achieve [6–9]. Most importantly, while an odd elastic solid would conserve linear momentum, it would, intriguingly, not be required to conserve angular momentum or energy. Odd elasticity has been widely studied for a range of applications, including self-locomotion of robots [10], localizing, attenuating and amplifying elastic waves in a non-Hermitian fashion [11, 12], biological systems [13, 14], active matters [15–17], and odd fluids [18].

The above theory and applications of odd elasticity have assumed, for theoretical studies [5, 11, 19–24] and both non-biological [10, 12, 25] and biological experimental studies [13, 26], the presence of an internal energy source, or electronic components coupled with feedback or robotic control [10, 12, 25] to enable the odd elastic behavior, and as such are considered variants of "active" odd elasticity. In contrast, the notion of driven odd elasticity was recently introduced [27], where the application of a periodic (driving) mechanical loading served as the input energy source to activate a theoretical non-reciprocal frictional response to enable a structure to exhibit an odd elastic response. This notion of driven odd elasticity is promising because external mechanical loading at the boundaries is the standard approach to applying forces on structures, and as such has the potential to enable odd elasticity in mechanical structures. However, exploiting driven odd elasticity still has an open challenge: the development of an internal mechanism, that does not require an internal energy source or electronic components, that causes a structure to respond non-reciprocally to applied loads. As such, to our knowledge, neither driven odd elasticity [27] nor the originally proposed odd elasticity [5] have been demonstrated in a mechanical system using only passive components and without electronic control or feedback systems.

Here, we demonstrate driven odd elasticity using passive components: a square lattice metamaterial, and chiral gears. Unlike known odd elastic media [10, 12, 13, 26] that have an internal source of energy (for biological active matter) [13, 26] or electronic components to achieve local feedback control [10, 12], we use driven chiral gears that act on the boundaries of the lattice metamaterial to achieve a non-reciprocal coupling between tension and shear. This results in the structure exhibiting an odd shear, whereby the application of normal strain results in shear strain, but the application of shear strain does not result in normal strain. This non-reciprocal coupling results in an asymmetric elasticity tensor, and we further demonstrate that the metamaterial reveals non-conservative work through a closed cycle of deformation. Finally, we observe that the non-reciprocal coupling between normal and shear deformation results in an effective anisotropic behavior of the system, which breaks parity-time (PT) symmetry and enables the emergence of the non-Hermitian skin effect [11].

A. Metamaterial design

We first introduce the components comprising the metamaterial. The first component, as shown in Fig. 1(a), is a gear with chiral teeth that is in contact with two horizontal walls. The gear, as well as the walls, have specific degrees of freedom described below but are not

* Department of Mechanical Engineering, Boston University, 02215, Boston, MA, USA
† parkhs@bu.edu

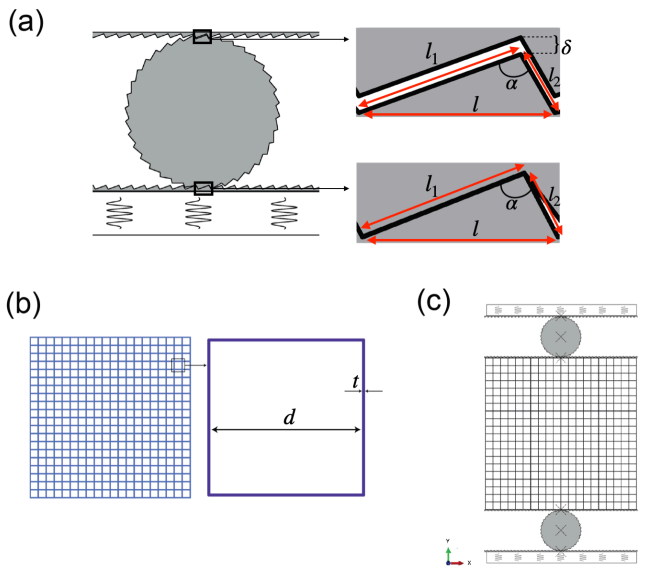

FIG. 1. (a) Chiral gears on springs, with geometry of gear contacts shown. (b) Square lattice metamaterial. (c) Coupled chiral gear plus metamaterial structure that exhibits driven odd elasticity.

deformable. The gear is already in contact with the bottom wall, while having a clearance of amount δ with the top wall. All surfaces in contact are assumed to have a coefficient of friction of $\mu = 0.1$, and long (l_1) and short (l_2) contact lengths. The top wall has a horizontal degree of freedom, while the bottom wall lies on a foundation with spring stiffness of k= 5×10^6 N/m that enables the bottom wall to move vertically, whereas the gear can both rotate and translate vertically. The specific dimensions for the results that follow are clearance δ=0.15 mm, teeth length l=3.5 mm and height h=1 mm.

The second component of the metamaterial is a square lattice with thickness t = 0.5 mm and unit cell length d=16mm as shown in Fig. 1(b), where each unit cell can stretch, shear and bend. We choose the mechanical properties of the metamaterial to be a Young's modulus of E=300 GPa, a Poisson's ratio of ν=0.3, and a density of ρ=8000 kg/m^3, to represent a generic class of metallic materials. As shown in Fig. 1(c), we then attach the gear mechanism in Fig. 1(a) to the bottom of the lattice metamaterial in Fig. 1(c), while the same gear structure in (a) is attached to the top surface of the lattice metamaterial by flipping it upside down in Fig. 1(c). The coupled mechanism plus metamaterial structure in Fig. 1(c) can then be driven by applying oscillatory motion of the gears. The importance of the gears having a chiral nature for the coupled gear plus lattice metamaterial to exhibit odd elasticity will be demonstrated next.

B. Mechanism for driven odd elasticity

We now demonstrate that the coupled gear plus metamaterial structure in Fig. 1(c) exhibits driven odd elasticity through finite element simulations using the commercial finite element software ABAQUS [28]. Within these simulations, we rotate (drive) the gears at a frequency of $\omega_d = 12\pi$, with amplitude $\Theta = 0.01$ radians, as shown in Fig. 2(a). This driven periodic oscillatory motion is analogous to the microscopic motions considered in the driven odd elasticity paper by Huang et al. [27], and we note that it could be achieved in both mechanical or non-mechanical means, for example through the torque generated by fluid flow interacting with rigid bodies [29, 30], or by the application of magnetic fields on bodies containing conductive materials [31]. Because of the initial contact between the gears and the walls on the elastic foundation, and because the top wall of the gear mechanism in Fig. 1(a) is tied to both the top and bottom surfaces of the lattice metamaterial as shown in Fig. 1(c), periodic rotation of the gears results in periodic shear forces being exerted on the metamaterial boundaries where the gears are attached.

While the driving periodic oscillatory motions are applied continuously to the gears, we also apply increments of normal strain $\Delta\epsilon_{yy}$ = 0.04% on the lattice as illustrated in Fig. 2(b). Importantly, when each increment of normal strain is applied, the gears momentarily lose contact with the metamaterial surfaces and are detached, as shown in Video 1. The clearance δ in Fig. 1(a) is critical here to enable space for the gear to detach as the normal strain is applied to the lattice. Once the gears regain contact with the walls, they do so at a new contact point, i.e. the *next* gear tooth position on the contacting horizontal wall. Because of the geometry of the horizontal walls in Fig. 1(a) (i.e. periodic repetition of gear teeth), this jumping of the gear from one tooth to the next locks in a new equilibrium position, and results in an increment of odd shear strain due to the application of the normal strain, and as such, the development of an odd shear stress. This is shown in Fig. 2(c), where we plot the shear stress as a function of time. There, we can see that each application of normal strain in Fig. 2(b) results in a corresponding increase in shear stress in Fig. 2(c).

Once we have applied each increment of normal strain, we allow the system to equilibrate at its new configuration (with both nonzero normal and shear strains) through continued application of periodic oscillatory motion of the gears, until the next application of normal strain. As can be seen in Fig. 2(c), the odd shear stress equilibrates about an equilibrium position before the next increment of normal strain is applied. Fig.2(d) shows the deformed metamaterial for different increments of normal strain, which shows that the position of the gears relative to the metamaterial boundaries shifts for each increment of normal strain relative to the undeformed state in Fig. 1(c), demonstrating the odd shear that has been generated through the application of the

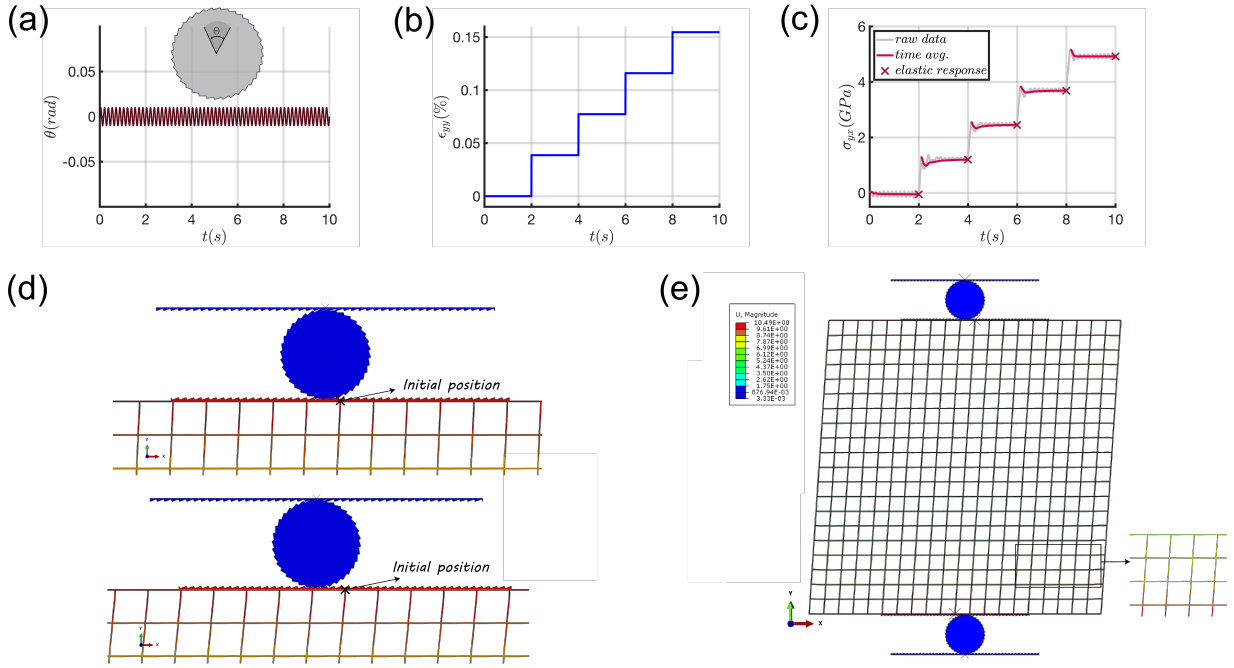

FIG. 2. (a) Illustration of periodic (driven) oscillations applied to each gear. (b) Normal strain increments ϵ_{yy} applied to the metamaterial. (c) Odd shear stress σ_{yx} resulting from each increment of normal strain ϵ_{yy} in (b). (d) The gears being displaced after two teeth (top), and four teeth (bottom) from its initial position. (e) Deformed configuration of the metamaterial after all normal strain in (b) has been applied demonstrating significant amount of odd shear deformation. The material properties are E=300 GPa and ν=0.3.

normal strain.

The chiral geometry of the gear teeth is important here, for several reasons. First, the asymmetric contact lengths l_1 and l_2 that are present in Fig. 1(a) mean that as the normal strain is applied, the lattice will be sheared in only one direction (i.e. in the direction normal to the larger contact length l_1). Second, as shown in the SI, larger normal strain increments are required to generate odd shear if the gear teeth are non-chiral (symmetric), both of which motivate the usage of the chiral gear geometry. In contrast, if the gear geometry is symmetric, then depending on the phase of the gear with respect to the wall that is tied to the metamaterial, the gear jump from the application of normal strain could result in the lattice being sheared in either direction, thus potentially cancelling any odd shear developed previously. The phase of the gear with respect to the wall tied to the metamaterial is also relevant for chiral gears. Specifically, because the chirality biases the lattice to be sheared in only one direction, application of normal strain can only result in either no jump (and no odd shear strain), or odd shear occurring in only one direction, depending on the phase of the gear with respect to the contact surface. The robustness of this mechanism with respect to the various geometric and material properties mentioned above for the metamaterial in Fig. 1(c) is discussed in detail in the SI.

Because the driving shear stress is periodic, to characterize the mechanical properties of the system, we study the time-averaged response of the system to the quasi-static normal strain ϵ_{yy} that occurs on the time scale $t = 2s$ as shown in Fig. 2(b), which is longer than the driving period $T = 2\pi/\omega$. As seen in Fig. 2(c), at each period, we measure the time-averaged shear stress, which converges to a constant after a few periods. This constant is the elastic response of the system, which we use to calculate the elasticity tensor C_{ijkl}, which relates the time-averaged stress σ_{ij} to strain ϵ_{ij}. The constitutive equation of this model is the following

$$\begin{bmatrix}\sigma_{xx}\\ \sigma_{yy}\\ \sigma_{yx}\\ \sigma_{xy}\end{bmatrix} = \mathbf{C}\begin{bmatrix}\epsilon_{xx}\\ \epsilon_{yy}\\ \epsilon_{yx}\\ \epsilon_{xy}\end{bmatrix} \tag{1}$$

where we write the 2D elasticity tensor as

$$\mathbf{C} = C^e + C^o = \begin{bmatrix}B+G & B-G & 0 & 0\\ B-G & B+G & 0 & 0\\ 0 & 0 & G & G\\ 0 & 0 & G & G\end{bmatrix} + \begin{bmatrix}0 & 0 & 0 & 0\\ 0 & 0 & 0 & 0\\ 0 & A & 0 & 0\\ 0 & 0 & 0 & 0\end{bmatrix} \tag{2}$$

In Eq. (2), B and G are the conventional bulk and shear moduli which are 214.3 and 115.4 GPa, respectively. However, A is an odd modulus coupling normal strain to shear stress. The elasticity matrix has symmetric and asymmetric (odd) parts $C = C^e + C^o$, where the symmetric part C^e is isotropic, whereas the asymmetric

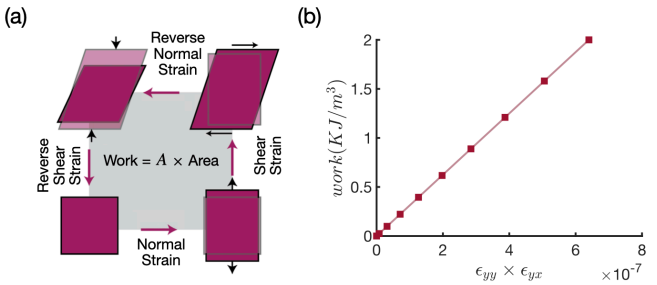

FIG. 3. Illustration of non-conservative work enabled by the odd elastic metamaterial in Fig. 1(c).

part C^o indicates normal strain causes shear stress, which establishes non-reciprocity in the system. We compute A as

$$A = \frac{\Delta\sigma_{yx}}{\Delta\epsilon_{yy}} \tag{3}$$

Using Eq. (3), we obtain $A = 3125$ GPa, which shows that a small increment of normal strain results in a significant odd shear stress. The amount of shear in each step is proportional to the length of the gear teeth l that are in contact (Fig. 1 (a)). This amount can be modified by geometric modifications, which is shown in the SI.

C. Statics

One important implication of an asymmetric (odd elastic) elasticity tensor is that a structure exhibiting that mechanical response can demonstrate non-conservative work through a cycle of deformations. We demonstrate this analytically by subjecting the metamaterial to a closed strain cycle of normal (ϵ_{yy}) and shear (ϵ_{yx}) strains according to Fig.3(a). The constitutive equations along this deformation path are

$$\begin{pmatrix}\sigma_{yy}\\ \sigma_{yx}\end{pmatrix} = \begin{bmatrix}B+G & 0\\ A & G\end{bmatrix}\begin{pmatrix}\epsilon_{yy}\\ \epsilon_{yx}\end{pmatrix} \tag{4}$$

The net work done in a closed deformation cycle is proportional to

$$\delta w = \sigma_{ij}\delta\epsilon_{ij} \tag{5}$$

For conventional elastic media, Eq. 5 is conservative, but this is not the case for odd elastic media, for which the work calculated through Eq. 5 has both conservative and non-conservative contributions, which can be written as

$$\begin{aligned}\delta w_p &= \frac{1}{2}\delta[(B+G)\epsilon_{yy}^2 + G\epsilon_{yx}^2]\\ \delta w_{np} &= A\epsilon_{yy}\delta\epsilon_{yx}\end{aligned} \tag{6}$$

The potential part δw_p is path-independent and vanishes in a closed deformation path. On the other hand, the non-potential part δw_{np} is path-dependent and remains non-zero at the end of the cycle, which leads to non-conservative work. Fig. 3(b) indicates that the work at the end of the cycle is proportional to the odd modulus A multiplied by the area of the strain cycle.

D. Dynamics

Odd elastic solids can also exhibit interesting dynamic properties, such as the non-Hermitian skin effect (NHSE), where due to the non-reciprocal constitutive relationships, modes will localize at the boundaries of the structure when open boundary conditions are enforced [11]. To consider this possibility in the driven metamaterial from Fig. 1(c), we derive the governing equations of motion. In odd elastic media, the linear momentum is conserved, and the forces are proportional to the divergence of the stress tensor.

$$\sigma_{ji,j} = \rho\ddot{u}_i \tag{7}$$

In Eq. 7, $\ddot{(\,)}$ represents a double derivative with respect to time, and ρ and u_j are the density and displacement, respectively. Substituting the constitutive relations in Eq. 1 into Eq. 7 leads to the two equations of motion that govern the dynamics of the system.

$$\begin{aligned}(B+G)\frac{\partial^2 u_x}{\partial x^2} + B\frac{\partial^2 u_y}{\partial x\partial y} + A\frac{\partial^2 u_y}{\partial y^2} + G\frac{\partial^2 u_x}{\partial y^2} &= \rho\ddot{u}_x\\ (B+G)\frac{\partial^2 u_y}{\partial y^2} + B\frac{\partial^2 u_x}{\partial x\partial y} + G\frac{\partial^2 u_y}{\partial x^2} &= \rho\ddot{u}_y\end{aligned} \tag{8}$$

The system has two degrees of freedom u_x and u_y and thus two equations of motion, where the odd modulus A appears in the second equation for $\ddot{u}_y$. We assume harmonic wave solutions $u_j = \hat{U}_j e^{i(q.x-\omega t)}$ for the discretized model of Eq. 8, where q is the wave vector. The dynamical matrix of Eq. 8 is non-Hermitian because of the odd modulus A, and this presence of A thus breaks PT symmetry in the x or y directions separately, implying the localization of eigenmodes at the edges. To find the eigenfrequencies of the system, we fix q_x and assume periodic boundary conditions in the y-direction. Due to the symmetry in the $x-$direction, we consider the Irreducible Brillouin Zone (IBZ), for which the spectrum comes in complex conjugate pairs for all $0 < q_x < \pi$. The eigenspectra of the periodic system are plotted in Fig. 4. It is observed that the frequency forms two closed bands that indicate the frequency in these regions is complex conjugate. For all the eigenfrequencies in these two bands, the corresponding eigenmodes are localized at the top and bottom edges of the metamaterial. Using the definition of the winding number, we can find the direction of the localization.

$$W(\omega_0) = \frac{1}{2\pi i}\sum_\alpha \oint_{-\pi}^{\pi} \frac{d}{dq}\log[\omega_\alpha(q) - \omega_0]\,dq \tag{9}$$

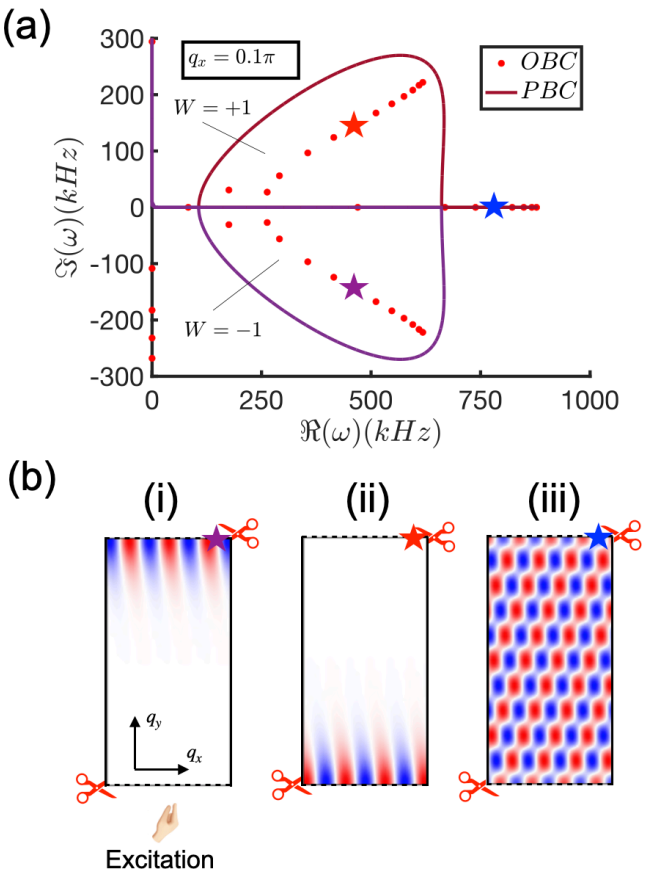

FIG. 4. (a) Spectrum for odd elastic metamaterial for both open and periodic boundary conditions. (b) Illustration of (i) amplified, (ii) attenuated, and (iii bulk) waves.

For every frequency in the upper band $W = +1$, whereas in the bottom band $W = -1$, which means that there is amplification in one direction and attenuation in the other direction. To visualize the eigenmodes of the system, we introduce open boundaries in the y-direction and solve the eigenvalue problem. Fig. 4(b) shows that in the presence of open boundaries, the wave is amplified in the bottom band (Fig. 4(b)(i)) and attenuated in the top band (Fig. 4(b)(ii)). Conversely, at the real-valued frequencies, we have bulk modes, as shown in Fig. 4(b)(iii).

In conclusion, we have demonstrated that driven odd elasticity is possible in a mechanical structure using only passive elements, namely chiral gears and a square lattice metamaterial. We achieve this leveraging periodic driving of chiral gears attached to the square metamaterial, where the chirality of the driven gears results in odd shear being developed when the metamaterial is subject to normal strains. We demonstrate that the resulting elasticity tensor is odd and asymmetric, which enables non-conservative work to occur in a cycle of normal and shear strains, and that the odd metamaterial exhibits unique dynamical responses, including the well-known non-Hermitian skin effect. We anticipate that the work presented here may motivate the development of other mechanisms in the future that can expand the scope and applicability of driven odd elasticity.

Both authors acknowledge the support of the AFOSR under award number FA9550-23-1-0299, while HSP also acknowledges NSF CMMI-2227474.

[1] M. Fruchart, C. Scheibner, and V. Vitelli, Odd viscosity and odd elasticity, Annual Review of Condensed Matter Physics **14**, 471 (2023).
[2] C. Coulais, D. Sounas, and A. Alu, Static non-reciprocity in mechanical metamaterials, Nature **542**, 461 (2017).
[3] J. D. Achenbach, *Reciprocity in elastodynamics* (Cambridge University Press, 2003).
[4] A. Montazeri, M. Rahimi, and H. S. Park, Non-reciprocity and asymmetric elasticity in twisting chiral metamaterials, International Journal of Mechanical Sciences **287**, 109990 (2025).
[5] C. Scheibner, A. Souslov, D. Banerjee, P. Surowka, W. T. M. Irvine, and V. Vitelli, Odd elasticity, Nature Physics **16**, 475 (2020).
[6] X. N. Liu, G. L. Huang, and G. K. Hu, Chiral effect in plane isotropic micropolar elasticity and its application to chiral lattices, Journal of the Mechanics and Physics of Solids **60**, 1907 (2012).
[7] I. Fernandez-Corbaton, C. Rockstuhl, P. Ziemke, P. Gumbsch, A. Albiez, R. Schwaiger, T. Frenzel, M. Kadic, and M. Wegener, New twists of 3d chiral metamaterials, Advanced Materials **31**, 1807742 (2019).
[8] X. N. Liu and G. K. Hu, Elastic metamaterials making use of chirality: a review, Journal of Mechanical Engineering **62**, 403 (2016).
[9] W. Wu, W. Hu, G. Qian, H. Liao, X. Xu, and F. Berto, Mechanical design and multifunctional applications of chiral mechanical metamaterials: a review, Materials and Design **180**, 107950 (2019).
[10] J. Veenstra, C. Scheibner, M. Brandenbourger, J. Binysh, A. Souslov, V. Vitelli, and C. Coulais, Adaptive locomotion of active solids, Nature **639**, 935 (2025).
[11] C. Scheibner, W. T. M. Irvine, and V. Vitelli, Non-hermitian band topology and skin modes in active elastic media, Physical Review Letters **125**, 118001 (2020).
[12] Y. Chen, X. Li, C. Scheibner, V. Vitelli, and G. Huang, Realization of active metamaterials with odd micropolar elasticity, Nature Communications **12**, 5935 (2021).
[13] S. Shankar and L. Mahadevan, Active hydraulics and odd elasticity of muscle fibres, Nature Physics **20**, 1501 (2024).
[14] D. Banerjee, V. Vitelli, F. Jülicher, and P. Surówka, Active viscoelasticity of odd materials, Physical Review Letters **126**, 138001 (2021).
[15] T. Markovich and T. C. Lubensky, Odd viscosity in active matter: Microscopic origin and 3d effects, Physical review letters **127**, 048001 (2021).
[16] T. H. Tan, A. Mietke, J. Li, Y. Chen, H. Higinbotham,

P. J. Foster, S. Gokhale, J. Dunkel, and N. Fakhri, Odd dynamics of living chiral crystals, Nature **607**, 287 (2022).

[17] Y.-C. Chao, S. Gokhale, L. Lin, A. Hastewell, A. Bacanu, Y. Chen, J. Li, J. Liu, H. Lee, J. Dunkel, *et al.*, Selective excitation of work-generating cycles in non-reciprocal living solids, Nature Physics , 1 (2026).

[18] C. Duclut, S. Bo, R. Lier, J. Armas, P. Surówka, and F. Jülicher, Probe particles in odd active viscoelastic fluids: How activity and dissipation determine linear stability, Physical Review E **109**, 044126 (2024).

[19] M. Shaat, Non-hermitian pseudo-gaps and higher-order skin modes in non-centrosymmetric, odd elastic solids, International Journal of Mechanical Sciences , 111103 (2025).

[20] Q. Wu, X. Xu, H. Qian, S. Wang, R. Zhu, Z. Yan, H. Ma, Y. Chen, and G. Huang, Active metamaterials for realizing odd mass density, Proceedings of the National Academy of Sciences **120**, e2209829120 (2023).

[21] Q. Wu, P. Shivashankar, X. Xu, Y. Chen, and G. Huang, Engineering nonreciprocal wave dispersion in a nonlocal micropolar metabeam, Journal of Composite Materials **57**, 771 (2023).

[22] W. Cheng and G. Hu, Odd elasticity realized by piezoelectric material with linear feedback, Science China Physics, Mechanics and Astronomy **64**, 114612 (2021).

[23] A. Lai, J. Zhou, and G. Fu, Odd elastic stability of cylindrical shells, European Journal of Mechanics-A/Solids **104**, 105220 (2024).

[24] D. Zhou and J. Zhang, Non-hermitian topological metamaterials with odd elasticity, Physical Review Research **2**, 023173 (2020).

[25] M. Brandenbourger, X. Locsin, E. Lerner, and C. Coulais, Non-reciprocal robotic metamaterials, Nature Communications **10**, 4608 (2019).

[26] T. H. Tan, A. Mietke, J. Li, Y. Chen, H. Higinbotham, P. J. Foster, S. Gokhale, J. Dunkel, and N. Fakhri, Odd dynamics of living chiral crystals, Nature **607**, 287 (2022).

[27] R. Huang, R. Mandal, C. Scheibner, and V. Vitelli, Odd elasticity in driven granular matter, Arxiv , 2311.18720 (2023).

[28] M. Smith, *ABAQUS Standard Users Manual, Version 6.9* (Dassault Systèmes Simulia Corp, United States, 2009).

[29] F. Mandujano and E. Vázquez-Luis, Chaotic vortex-induced rotation of an elliptical cylinder, Chaos: An Interdisciplinary Journal of Nonlinear Science **34** (2024).

[30] D. Bonheure, G. P. Galdi, and C. Patriarca, Forced oscillations of a spring-mounted body by a viscous liquid: rotational case, Pure and Applied Analysis **7**, 1209 (2025).

[31] K. Polczyński, M. Bednarek, and J. Awrejcewicz, Dynamics of pendulum forced by a magnetic excitation with position-dependent phase, in *International Conference on Nonlinear Dynamics and Applications* (Springer, 2024) pp. 327–337.